Direct olivine carbonation: Optimal process design for a low-emission and cost efficient cement production

Andreas M. Bremen,[†] Till Strunge,[‡,¶] Hesam Ostovari,[§] Hendrik Spütz,[†] Adel Mhamdi,[†] Phil Renforth,[‡] Mijndert van der Spek,[‡] André Bardow,[§,‖,⊥] and Alexander Mitsos[*,†,‖,#]

†*Process Systems Engineering (AVT.SVT), RWTH Aachen University, 52074 Aachen, Germany*

‡*Research Centre for Carbon Solutions, School of Engineering and Physical Sciences, Heriot-Watt University, Edinburgh EH14 4AS, United Kingdom*

¶*Institute for Advanced Sustainability Studies e.V., 14467 Potsdam, Germany*

§*Institute of Technical Thermodynamics, RWTH Aachen University, Aachen, Germany*

‖*Institute of Energy and Climate Research: Energy Systems Engineering (IEK-10), Forschungszentrum Jülich GmbH, 52425 Jülich, Germany*

⊥*Energy & Process Systems Engineering, ETH, 8092 Zurich, Switzerland*

#*JARA-ENERGY, 52056 Aachen, Germany*

E-mail: amitsos@alum.mit.edu

Abstract

Employing mineral carbonation products as a cementitious substitute could reduce the cement industry's greenhouse gas emissions. Yet, a transition towards low-emission cement requires financially competitive cement production at standardized product

specifications. Aiming to tackle this challenge, we modeled and optimized a direct mineral carbonation process. In detail, we embedded a mechanistic tubular reactor model in a mineral carbonation process and imposed product specifications based on the European cement standard in the optimal design formulation. In the next step, we considered the business case of blended cement consisting of ordinary Portland cement and the mineral carbonation product that could be categorized as CEM II in the European cement standard. We computed the minimum production cost and greenhouse gas emissions of the produced blended cement by using Bayesian optimization to find Pareto optimal operating conditions of the mineral carbonation process. Our results showed that the cost of mineral carbonation in the cement industry can be competitive while cutting the greenhouse gas emissions up to 54 %.

1 Introduction

The cement industry is required to reduce greenhouse gas (GHG) emissions both resulting from energy-related CO_2 emissions and process-inherent CO_2 emissions caused by the calcination of limestone ($CaCO_3$).[1,2] A decrease of the energy-related CO_2 emissions requires a shift towards renewable energy supply and improvements in energy efficiency.[2–7] Yet, reducing the CO_2 emissions from calcination necessitates the reduction of cement's clinker intensity or the installation of carbon capture and storage (CCS).[3,8–12] Mineral carbonation can both reduce cement's clinker intensity and the direct CO_2 emissions by chemically binding CO_2 from the flue gas of cement production and using mineral carbonation products to partially substitute clinker.[2,13–16] Mineral carbonation products are mineral carbonates and amorphous silica. Benhelal et al.[16] have shown the applicability of amorphous silica from mineral carbonation as supplementary cementitious material (SCM) by experimentally comparing compressive strengths of mortars composed of ordinary Portland cement (OPC) and different amounts of amorphous silica. The blended cement containing clinker and SCM from mineral carbonation could become carbon-neutral under certain circumstances, e.g.,

with a high substitution rate and a large amount of low-emission electricity.[2] However, the economic feasibility of operating a mineral carbonation plant requires closer consideration. Especially for a standardized commodity such as cement, cost factors play a significant role. A business case is viable, only if the production of blended cement becomes profitable.[15]

Previous studies focus mainly on the assessment of mineral carbonation in terms of the amount of stored CO_2.[17–21] Hitch and Dipple[22] used synergies of mining and mineral carbonation in their economic study on the use of waste streams containing magnesium silicates for mineral carbonation. In a recent study on the economic feasibility of blended cement with by-products from mineral carbonation, we concluded that blended cement can compete with conventional OPC on the basis of potential revenue from the European emission trading system (ETS),[15] but the gap between a substantial greenhouse gas emission reduction and costly mineral carbonation remains. Additionally, only precipitated calcium carbonates are currently granted ETS eligibility,[23] while a similar decision is expected for magnesium carbonates.[15] In summary, to reduce the cement industry's greenhouse gas emissions via mineral carbonation, both the utilization of silica-rich SCMs in the production of blended cement as well as the eligibility of mineral carbonation in the ETS are required.

Generally, recent studies on the sustainability and profitability of mineral carbonation processes rely on assumptions of operating conditions and conversion rates based on experimental results.[2,14,15] Estimating process performance from experiments is a suitable approach within the scope of evaluating the potential of technology. However, this procedure limits the scope to distinct operating conditions used in experiments. We previously performed sensitivity analyses for different operating conditions but had to neglect their dependency on conversion rates, as experimental results are only available for distinct operating conditions.[14,15] Therein, the evaluated process configurations refer to direct and indirect mineral carbonation, which employ a single reactor or spatially separated reactors for dissolution of feedstock and precipitation of product, respectively. We concluded that the direct mineral carbonation of olivine shows the greatest potential in Europe based on the limited availability

of experimental data.[2,14,15]

Several experimental studies have determined beneficial operating conditions for direct mineral carbonation of olivine.[19,20,24–31] These studies assessed conversion rates depending on temperature, pressure, additives, and particle size of feedstock material. According to Gerdemann et al.,[20] optimal operating conditions for the direct olivine carbonation are at a temperature and pressure of 185 °C and 150 bar, respectively.[20] Gerdemann et al.[20] showed experimentally that at 185 °C conversion is at a maximum and argued that pressure above 150 bar is impractical. Eikeland et al.[28] reported a maximum conversion at 190 °C at a pressure set to 100 bar. They suggested that a particle size $< 10\,\mu m$ is preferable. Wang et al., Wang et al.[30,31] performed experiments at moderate pressure (< 45 bar) with an optimal temperature of T = 175 °C. Thus, lab-scale experiments indicate a pressure-dependent optimal temperature, whereas a trend is not clear. To quantify these dependencies, we developed a dynamic, mechanistic model of direct forsterite carbonation that accounts for reaction kinetics.[32] The model is capable of predicting conversion rates on the basis of model inputs: temperature, pressure, and particle size. Therein, we formulated dynamic mole balances and applied nonideal thermodynamics for the species interaction. Hence, the influence of operating conditions of the reactor, i.e., temperature, pressure, particle size, and residence time are extensively evaluated with respect to reactor performance, both experimentally and computationally.[19,20,24–32] However, these process design choices require the consideration of the overall mineral carbonation process to obtain (1) favorable operating conditions for (2) a low-emission and cost-efficient process configuration.

Up to now, mineral carbonation research is only driven by the need for GHG emission reduction, as the economic performance of large-scale mineral carbonation is evaluated as means of cost of CO_2 storage.[14,17–20,22] The main issue of previous studies on operating conditions, life-cycle, and techno-economic assessments of mineral carbonation is their inability to holistically investigate the multi-objective nature of this problem, i.e., both sustainability and profitability. In this study, building on previous work,[2,15,32] we combine mechanistic

reactor modeling and process modeling with life cycle and techno-economic assessment to evaluate the implementation of mineral carbonation in the cement industry. For this purpose, we aim at finding the optimal operating conditions and process scale for the direct mineral carbonation of olivine in terms of GHG reduction and profitability of blended cement.

In this study, we propose a process design including pretreatment, reaction, and separation steps, given in Section 2.1. In Section 2.2, we reformulate the balance equations of a mechanistic batch carbonation model[32] to a tubular reactor model to predict reactor performance depending on operating conditions. Subsequently, in Section 3, we propose evaluation criteria by introducing the carbon footprint and the levelized cost of blended cement at predefined composition on the basis of models taken from Ostovari et al.[2] and Strunge et al.,[15] respectively. With these criteria, we optimize the reactor conditions and the process scale by the use of Bayesian optimization[33] for a present time and a future scenario in Section 4. This enables both the evaluation of process operating conditions as well as the simultaneous consideration of environmental and economic benefits. Finally, in Section 5, we close with concluding remarks. With this work, we close the gap between the evaluation of distinct process set-ups and the determination of optimal operating conditions for a low-emission and profitable cement production.

2 Industrial-scale olivine carbonation process

Previous research on the performance of mineral carbonation focuses on lab-scale experiments. However, its industrial scale-up imposes major challenges. The combination of large process streams and long residence times due to slow reaction kinetics results in large process units. Additionally, the low added value in a mineral carbonation process requires a smart choice of recycling streams to minimize the loss of valuable auxiliary streams.

Generally, a direct mineral carbonation process comprises three steps: pretreatment, reaction, and separation (cf. Section 2.1). The first step includes crushing and grinding of

mined feedstock material and the supply of purified CO_2 from the flue gas. In the second step, the mineral reacts with CO_2 to form carbonates and amorphous silica. Finally, in the separation step, the carbonation products, the unreacted feedstock, and the liquid phase are separated and partially recycled.

For the pretreatment step, i.e., the grinding of feedstock and purification of CO_2, we assume the state-of-the-art technology for the direct mineral carbonation of olivine as applied in our previous studies.[2,14,15] Previous studies on industrial-scale mineral carbonation considered continuously stirred tank reactors (CSTR), as they seem viable from a lab-scale experimental perspective.[2,14,15,19,34] However, the long residence times and large process streams necessitate a large number of CSTRs. Therefore, O'Connor et al.[19] proposed a tubular reactor with a CO_2 side-feed but did not include this set-up in their economic and environmental evaluation. Our study is the first to consider the use of tubular reactors for mineral carbonation in the process design. We compute reactor outlet properties by the use of mechanistic modeling of tubular reactors as discussed in Section 2.2.

The basis for the separation of the reactor outflow is taken from our previous work,[15] where we adopted the process conditions from Eikeland et al.[28] and use findings for solid separation from Kremer and Wotruba.[35] Here, we extend the solid separation sequence to achieve defined product specifications based on the particle size distributions (PSDs) of solid phases at the reactor outlet that are computed with the mechanistic reactor model. In detail, the design of the solid separation enables customized silica content in the product stream. In our case, we assume that particles do not interact with each other, i.e., they do not coagulate, as the unit operations and their implications on particle interaction are yet subject to research.[35] As such, we do not have enough information to account rigorously for potential interactions. Our calculations are in that sense idealized, i.e., what reactor design should aim for. Still, Kremer and Wotruba[35] consider hydrocyclones and classification centrifuges as promising unit operations for high separation efficiencies at high throughput but mention the need for further research. Hence, we here consider hydrocyclones and classification

centrifuges in the separation sequence for the separation of the unreacted olivine, and the product phases (magnesite and amorphous silica) on the basis of density difference and different PSDs of solid phases. Furthermore, to obtain an energy-efficient process, we adopt the results from the heat integration in our previous work.[2,14]

In Section 2.1, we guide through the proposed process design and justify major assumptions. Subsequently, in Section 2.2, we give the foundation for the incorporation of a tubular reactor in the process design based on our mechanistic reaction model.[32] Finally, we provide detail on the process model implementation and simulation in Section 2.3.

2.1 Olivine carbonation process design

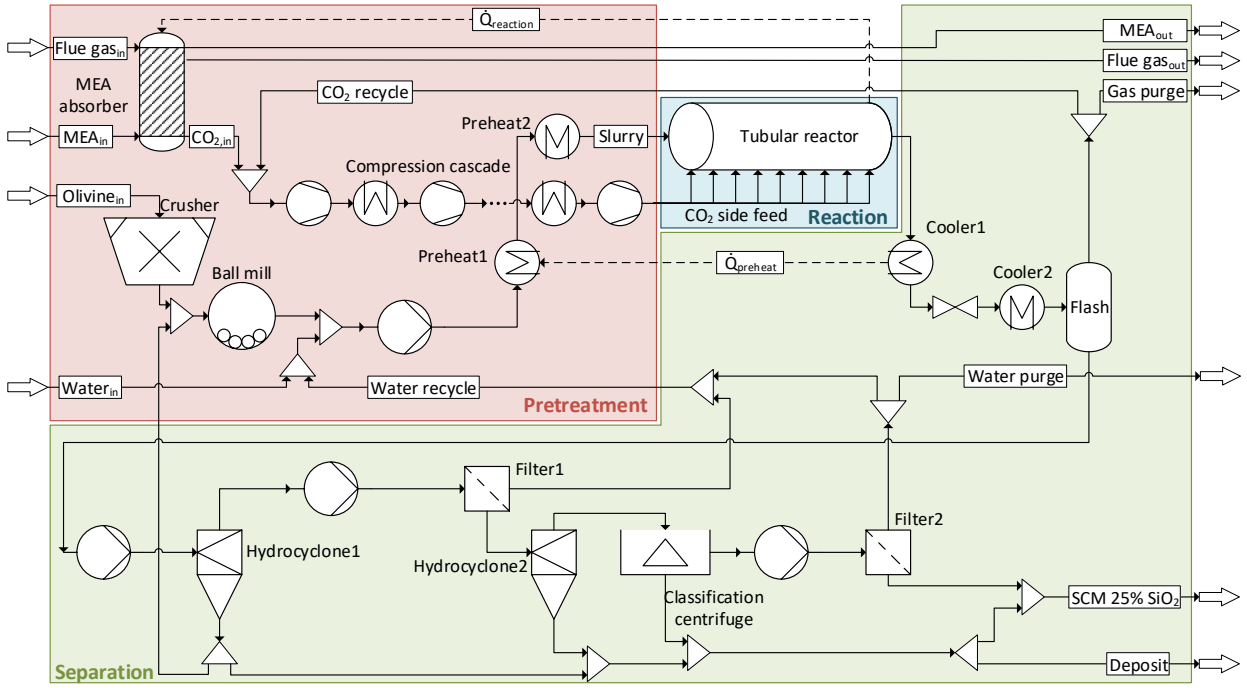

Figure 1: Direct mineral carbonation process divided into the pretreatment (□), reaction (□), and separation (□) with mass streams (——) and heat streams (- - -).

Fig. 1 shows the flowsheet of the mineral carbonation process. The mineral feed to the process is olivine, which comprises roughly 80 % forsterite (Mg_2SiO_4) and 20 % fayalite (Fe_2SiO_4).[36–38] We assume only carbonation of forsterite while fayalite is inert. In the pretreatment step, the solid pretreatment set-up is taken from O'Connor et al.[19] consisting of

two particle size reduction steps. The feedstock mineral is first pretreated in a cone crusher to obtain a particle size $< 1\,\mathrm{cm}$ and then mixed with a recycled mineral stream. A ball mill provides the desired PSD of feedstock material for carbonation. We assume a normal distribution with a mean diameter μ_{olivine} and standard distribution $\sigma_{\mathrm{olivine}} = \frac{\mu_{\mathrm{olivine}}}{6}$. We estimate the power requirement for fine grinding from the surface area increase and a mineral-specific surface tension combined with a grinding efficiency of $1\,\%$.[39] The ground solid material mixed with partially recycled process water is then pressurized to the reaction pressure. Subsequently, the stream is preheated with the reactor outflow up to a temperature of $T_{\mathrm{Preheat1,out}} = T_{\mathrm{reaction}} - \Delta T_{\mathrm{min}}$ where T_{reaction} is the reaction temperature and ΔT_{min} is the minimum temperature difference of $10\,^{\circ}\mathrm{C}$. Steam then heats the slurry to the reaction temperature in *Preheat2* before the slurry enters the tubular reactors.

Similar to previous studies,[2,14,15] we consider monoethanolamine (MEA) post-combustion capture to obtain purified CO_2 from the cement plant's flue gas stream. The MEA post-combustion capture, represented as a single unit in Fig. 1, requires (a) the solvent MEA as makeup stream, (b) heat provided by the reaction enthalpy from the reactors ($\dot{Q}_{\mathrm{reaction}}$), and (c) steam as an external utility. Both the MEA makeup and required heat depend solely on the amount of the purified CO_2 feed to the process $CO2, in$. After purification, the CO_2 is pressurized in a compression cascade with intercooling. Then, the CO_2 stream is stoichiometrically fed to the tubular reactor through a side feed to keep the gas volume flow within the reactor constant. The number of tubular reactors depends on the scale of the process and resulting mass flow at the reactor inlet. Section 2.2 provides further details on the reactor assumptions.

In the separation step, the reactor outflow is cooled down and expanded to ambient conditions to separate the unreacted CO_2 in the flash unit for recycling. The solid-liquid slurry is processed by (1) separating unreacted olivine in *Hydrocyclone1* for recycling, (2) separating remaining large particles consisting of olivine and magnesite in *Hydrocyclone2* and the *Classification centrifuge*, and (3) filtering excess process water in *Filter1* and *Filter2*. The

use of *Hydrocyclone1* for olivine recycling is adapted from Strunge et al..[15] The recycled mineral stream contains an increased content of inert material. Thus, we limit the recycling stream to allow at most a 30 % share of inert material at the reactor inlet. The subsequent separation of product phases is particularly designed for the separation of particle size distributions obtained from the mechanistic reactor model. In detail, we employ the additional *Hydrocyclone2* to enable sufficient purification of the product phase in the *Classification centrifuge* that is adapted from Strunge et al..[15] Instead of using a dewatering centrifuge as in Strunge et al.,[15] we employ filters that do not contain any solid phase in the permeate to prevent the recycling of product phases. The solid product streams are partially mixed to obtain a product stream containing a 25 % content of amorphous silica. The solid streams contain residual moisture of 10 %. This separation sequence enables the process to provide SCM with the predefined amorphous silica content for the range of operating conditions employed in this study. As the unit operations in the separation sequence have only a minor influence on costs and GHG emissions, potential design changes required due to different solid phase specifications, e.g. by particle interaction, are expected to have a limited impact on the evaluation of the overall system.

2.2 Mineral carbonation tubular reactor

Tubular reactor models have different levels of accuracy based on mechanistic effects that are considered. The most detailed variant are three-dimensional distributed models considering convective and diffusive fluxes resulting in partial differential equations (PDE) that require suitable boundary conditions. The effects along the axial direction of the reactor, i.e., reaction progress, are much more decisive for the evaluation of olivine carbonation performance than effects in the azimuthal or radial direction. Furthermore, the technological readiness level of mineral carbonation does not allow such detailed modeling as up to now, experimental investigations were only conducted in batch operation.[19,20,24–31] Additionally, the investigations did not focus on understanding mechanistic effects within the mineral car-

bonation system such as mass transfer at phase boundaries, particle interaction, diffusion effects, and flow regimes throughout the reaction. Thus, rigorous reactor modeling under consideration of all mechanistic effects is still not possible. Hence, a simpler model for the feasibility of a tubular reactor for mineral carbonation is the only option without detailed experimental investigations, which go beyond the scope of this study. Furthermore, disregarding the radial and azimuthal dependence of the reactor yields computationally faster performance. As the reaction conditions change substantially along the axial direction, we do consider this dimension. We assume stationary operation, resulting in differential equations with a single independent variable. Most importantly, our model predicts what reactor design should aim for, i.e., the best possible performance as we disregard potential mass transfer limitation in azimuthal and radial direction.

In the following, we first analyze the reactor dimensions in combination with flow regimes and, subsequently, we consider the underlying mineral carbonation reaction system. We illustrate the tubular reactor cross-sectional area to highlight the multi-phase flow in Fig. 2 and provide the considered data for the calculations in Appendix A.

To design a tubular reactor for the direct carbonation of olivine, we consider the potential size (length, diameter) of a tubular reactor as well as flow regimes of the multi-phase flow. For this purpose, we consider a multi-phase mixture of olivine, water, and CO_2 at reactor temperature and pressure set to 185 °C and 150 bar, respectively. These values are reported as favorable reactor conditions for the carbonation of olivine.[19] For the analysis, we provide substance properties at reactor conditions summarized in Appendix A Tab. 2. We estimate the properties of the slurry as a quasi-homogeneous phase that contains water and olivine based on Thomas,[40] who provided a correlation of dynamic viscosity and solid volume fractions up to 50 % under consideration of non-Newtonian, inertial and non-homogeneous suspension effects.

In this study, we adopt the solid/liquid ratio of $0.2\,\mathrm{kg_{olivine}/kg_{water}}$ from previous studies.[15,32,41] With its lower density, the suspension carrier solution (water) takes up a major

share of the volume. In combination with a residence time of 3 h taken as average from multiple experimental studies,[19,28,30,31,41] a large reactor volume is required. As pressurized tubular reactors come with construction limitations at large sizes (e.g., due to statics requirements), following Aspen Capital Cost Estimator,[42] we limit the reactor diameter and length to 1.25 m and 120 m, respectively. With these maximum dimensions, we employ multiple reactors to obtain sufficient reactor volume for an industrial scale carbonation process. The required reactor volume could be realized in parallel operation or with multiple reactors in series. The parallel configuration enables the straightforward evaluation of the process scale as the number of identical reactors can be selected according to the required reactor volume, while the flow properties in each reactor remain the same. In the following, we analyze the flow properties of one tubular reactor with a diameter of 1.25 m and a length of 120 m. In the overall process, we employ several such tubular reactors.

At constant fluid density, the maximum overall volume feed flow rate is $1.36 \times 10^{-2} \frac{\mathrm{m}^3}{\mathrm{s}}$ corresponding to the given residence time. Besides the slurry flow, a gas phase flow needs to be fed into the reactor to supply CO_2 for the carbonation reaction. If a stoichiometric CO_2 gas feed solely entered at the reactor inlet, the gas phase would take up more than 50 % of the cross-sectional area resulting in an even larger reactor volume. Hence, as O'Connor et al.[19] proposed, we employ a CO_2 side feed at the reactor bottom so that the gas phase disperses within the solid-liquid slurry. The CO_2 feed is stoichiometric so that the gas volume flow occupies 10 % of the cross-sectional area at all axial positions. To maintain a residence time of 3 h, the olivine feed flow rate is limited to $2 \frac{\mathrm{kg}}{\mathrm{s}}$ resulting in an overall volume feed flow rate (gas-slurry) at the reactor inlet of $13.6 \frac{\mathrm{m}^3}{\mathrm{s}}$.

Depending on the mass flow rate and phase properties (density, viscosity) of the gas and slurry flow, different flow patterns occur in a pipe flow.[43] We calculate the required flow properties for both phases for the determination of the flow pattern (cf. Appendix A, Tab. 3), and find a stratified flow pattern with separate gas (top) and slurry (bottom) flows. This flow pattern may prohibit sufficient mixing and, hence, may result in a limited mass transfer

at the gas-liquid interface. As compensation, the CO_2 side feed at the reactor bottom further enables dissolution of gaseous CO_2 in the slurry, as illustrated in Fig. 2. In our study, we do not consider, however, the gas bubbles within the slurry in the analysis of gaseous flow properties and consider the flow of the gas phase on top of the slurry phase only.

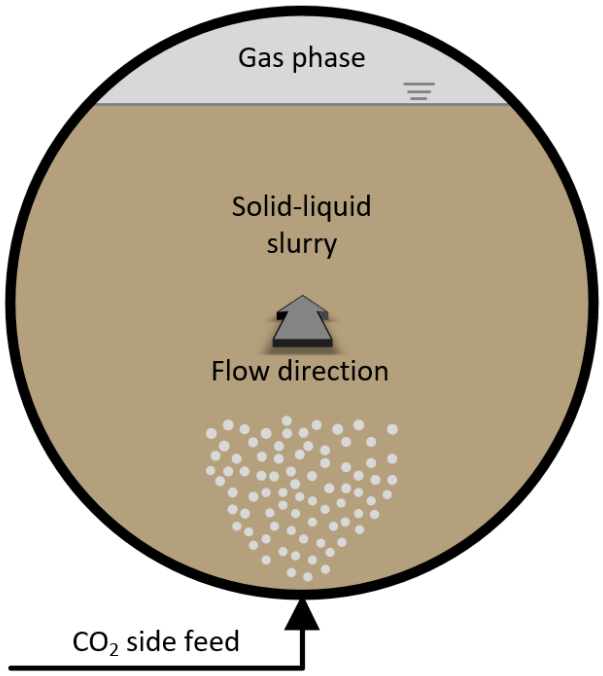

Figure 2: Cross sectional area of the plug flow reactor with CO_2 side feed at reactor bottom and multi-phase flow of gas phase and solid-liquid slurry. The stratified flow profile of slurry and gas phase is justified with the two-phase tubular flow analysis by Baker.[43]

Due to the non-circular cross-sectional area of gas and slurry flows, the analysis of the flow regime of the slurry flow and the gas flow requires the consideration of the hydraulic diameter. It enables the calculation of flow properties assuming a tubular flow of this diameter. With the hydraulic diameter, we obtain a turbulent flow of both the slurry and the gas flow with $Re_{\text{slurry}} = 4.9 \times 10^4$ and $Re_{\text{gas}} = 2.4 \times 10^4$ denoting the ratio of inertial forces to viscous forces. With the turbulent flow of the slurry phase, we evaluate the effects of axial mixing by the consideration of axial dispersion. In general, axial dispersion is caused by molecular diffusion, nonideal flow profiles, and in the case of turbulent flow, turbulent diffusion (eddies).[44] We estimate the dispersion coefficient in a turbulent pipe flow

of the quasi-homogeneous slurry from a correlation of Reynolds number, flow velocity, and hydraulic diameter to be $E = 2.2 \times 10^{-3} \frac{\mathrm{m}^2}{\mathrm{s}}$.[45] Taylor[45] considers the effects of a nonideal flow profile and turbulent diffusion with the former being the dominant factor for dispersion in a turbulent flow. To account for molecular diffusion, we consider the H^+ ion as the smallest molecule in our system and, hence, the highest diffusion coefficient reported as $D_{H^+} = 9.3 \times 10^{-9} \frac{\mathrm{m}^2}{\mathrm{s}}$.[46] With $D_{H^+} \ll E$, the consideration of axial molecular diffusion is negligible. Hence, to determine the effects of axial dispersion in comparison to convective flow, axial dispersion by turbulent diffusion and nonideal flow profile is sufficient. We determine the Bodenstein number of the slurry flow to be $Bo_{\mathrm{slurry}} = 611$ which denotes the ratio of convection to dispersion. With $Bo \gg 1$, we can neglect axial dispersion in the slurry flow and, thus, assume no mixing of slurry in the axial direction. The gas phase contains CO_2 and H_2O, and its composition remains nearly constant over the reactor length. The gas phase is assumed to be in equilibrium with the liquid phase, whose change in composition over the reactor length only slightly affects the gas phase composition at constant temperature and pressure. Hence, dispersion effects are irrelevant in the gas phase.

We point out that we do not consider radial mixing effects of the top gas phase and gas bubbles within the slurry since this would entail a thorough analysis of, among other factors, bubble size, buoyancy velocity, the interaction of gas bubbles with solid particles, and gas-liquid phase, all in a turbulent slurry flow. Instead, we assume a best-case scenario with ideal mixing in this work and leave these points open for future research. Hence, based on this analysis we assume a one-dimensional convective flow profile (plug flow) of both the gas phase and the slurry without consideration of axial dispersion and diffusion for the range of reactor operating conditions.

To model a plug flow reactor, we extend the mechanistic reaction model from our previous work[32] to a convective reactor model. The original model is a system of differential and algebraic equations (DAE) that accounts for (1) the isopotential conditions of gas-liquid equilibrium (GLE) and the law of mass action for dissociation equilibrium (DE), (2) surface-

controlled dissolution and precipitation of solid phases coupled with nucleation of product phases and (3) PSDs of solid phases. The DAE is of a differential index higher than one due to the consideration of isopotential conditions. Therefore, the mole balance equations are projected to reaction invariants to obtain a DAE of differential index one.[47–50] In our previous work, we showed similarities to batch experiments underlining the model capabilities of predicting mineral carbonation performance.[32] For the conversion of the transient batch reaction model to a stationary plug flow reactor model, we replace the projected mole balance equations of the original model with projected balance equations for one-dimensional convective flow. For further details on governing and constitutive equations, thermodynamics, and model assumptions, we refer to Bremen et al..[32]

2.3 Process implementation and simulation

The process model (mass and energy balances) and the reactor model are implemented in Aspen Plus V11[51] and Dymola 2020,[52] respectively. Based on the modeling language Modelica,[53] Dymola is a widely used software environment for the object-oriented modeling of complex systems with a wide range of applications. With open-source software environments, Modelica allows the reusability of model components and enables interfacing with control and dynamic optimization software.[54] The simulation of the entire process requires the results of the Dymola simulation to be provided to the Aspen model. For this purpose, we use a Matlab[55] interface to both Dymola and the Aspen Simulation Workbook (ASW). The ASW is provided in MS Excel[56] that links Aspen Plus flowsheet variables. As the process simulation depends on the reactor outputs, we run the plug flow reactor model first with given operating conditions: temperature, pressure, and particle size distribution. To integrate the Dymola model, we provide model inputs (temperature, pressure, feedstock particle size distribution) and use the DAE integrator DASSL[57] with an integration tolerance of 10^{-8}. After running the reactor model, we extract simulation results and provide these as input to the ASW, namely the overall conversion, PSDs of solid phases, and the required

feed of CO_2. The simulation results of the process model in Aspen Plus are then used for the evaluation of the process described in the following Section 3.

3 Olivine carbonation process assessment

To analyze the mineral carbonation process proposed in Section 2.1, we provide the setting and major assumptions for the evaluation in Section 3.1 and briefly summarize criteria for cost and carbon footprint assessments in Sections 3.2 and 3.3, respectively. In this work, we consider both a present-day scenario (2021) and a future scenario (2030) further detailed in Section 3.4. The underlying model equations are implemented in Matlab.[55] We provide parameters for the techno-economic assessment and the life cycle assessment (LCA) that differ in both scenarios in Appendix B. For remaining parameters, we refer to Strunge et al.[15] and Ostovari et al..[2] All parameters are also provided within the models given the electronic supplementary information (ESI).

3.1 Scope of this study

The aim of the mineral carbonation process is to produce SCM via the direct carbonation of olivine while storing sufficient CO_2 to reduce the carbon footprint of the cement industry, as shown in Fig 3. The European cement standard allows different amounts of SCM of certain compositions to replace OPC and categorizes different cement types depending on OPC substitution.[58] CEM II is the most consumed type of cement in Europe consisting of OPC mixed with different shares of shale and silica fume, fly ash, limestone, natural pozzolan, and/or steel slag.[59,60] The European cement standard DIN EN 197-1[58] defines a CEM II to contain 20-35 wt.% natural pozzolan with at least 25 wt.% amorphous silica that is the strengthening component in blended cement. In our study, we aim to produce SCM from mineral carbonation that performs as a natural pozzolan. Therefore, 25 wt.% of the SCM should be silica while magnesite and unreacted olivine are the remaining components

(see Fig. 1). We assume the average allowed substitution of 27.5 wt.% as a representative substitution rate.

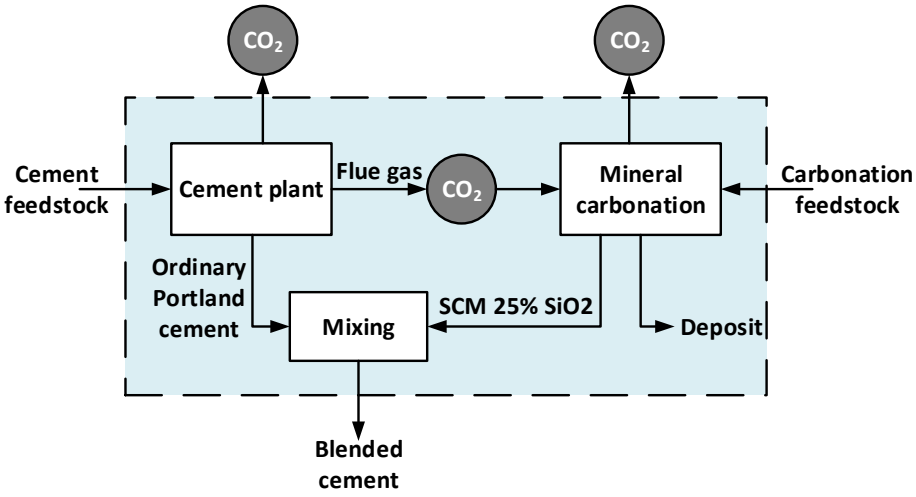

Figure 3: The mineral carbonation plant produces SCM with CO_2 from the cement plant. OPC and SCM are then mixed to produce blended cement.[2]

The mineral carbonation process is assumed to be located next to a cement plant in central Europe that produces one million tons of OPC per year with emissions of 850 $\mathrm{kg_{CO_2}/t_{OPC}}$.[61] This enables a potential OPC substitution by SCM of 275,000 $\frac{\mathrm{t}}{\mathrm{a}}$. Further mineral carbonation products are deposited in the limestone quarry close by to the cement plant (10 km). As suitable feedstock mineral is located in Southern and Northern Europe,[38,62] we transport raw material a distance of 1200 km to the production site, partially by ship, train, and truck.

3.2 Techno-economic assessment

The economic evaluation is adapted from Strunge et al.,[15] who built a business case based on (a) the usage of mineral carbonation product streams as SCM, (b) ETS eligibility of the CO_2 avoidance, and (c) feedstock availability in relatively close proximity (< 2000 km). The economic model considers both capital expenditures (CapEx) and operational expenditures (OpEx) for the construction and operation of the mineral carbonation plant. To obtain a single evaluation criterion, we introduce the levelized cost of blended cement that includes

participation in ETS, OpEx, and discounted CapEx using an expected plant lifetime at a given interest rate.

The production of blended cement emits CO_2, thus requiring participation in the ETS. The ETS prices depend on the considered scenario setting discussed in the subsequent process optimization (Section 3.4). OpEx constitutes expenditures for feedstock supply and transport, cooling water, electricity, steam, product deposit, insurance, labor, and maintenance.

We calculate the CapEx by estimating the expected cost of a mature technology based on an n^{th} of a kind plant.[63,64] The CapEx further constitutes the total direct cost of each process unit taking indirect costs, process contingencies, and project contingencies into account. Total direct costs are given in Aspen Plus Capital Cost Estimator[51] for the compressors, pumps, heat exchangers, flash unit, expanders, hydrocyclones, filters, and the classification centrifuge. We take total direct cost functions for the units MEA post-combustion capture, cone crusher, ball mill, and tubular reactors from Strunge et al..[15] The crusher and ball mill are sized according to their power input. The electricity demand of the crusher is set to a value of $2\,\frac{\mathrm{kW\,h}}{\mathrm{t}}$[20] with a constant output particle size. The ball mill power demand is proportional to the specific surface area increase, and therefore dependent on the predefined output particle size distribution.[39]

3.3 Life cycle assessment

Our study is based on the LCA method described in ISO 14040, ISO 14044 and ISO 14067.[65–67] As our main motivation for mineral carbonation is the reduction of GHG emissions, we focus on its impacts on climate change by applying the standardized methodology of carbon footprinting.[67] The carbonation process stores the CO_2 from the flue gas of cement production and avoids GHG emission by substituting clinker. Yet, the construction and operation of the plant cause GHG emissions due to material and energy demand. To reduce the carbon footprint of cement, the carbonation process should emit less GHG emissions

than it avoids.

To assess the GHG emissions from the mineral carbonation process, we use data from Ostovari et al..[2,14] In detail, we account for GHG emissions from carbonation plant construction, mining, transportation, consumption of feedstock, cooling water demand, electricity demand, thermal energy demand, and product deposit. We assume the GHG emissions from carbonation plant construction to be proportional to the amount of treated CO_2. To calculate the carbon footprint of SCM, we subtract the overall stored CO_2 from the GHG emissions caused by the mineral carbonation process. Thus, we provide a credit for the CO2 emissions avoided from the flue gas in line with the recommendations of Müller et al..[68] The carbon footprint of blended cement is the sum of the carbon footprint of SCM and of OPC with the predefined shares of 27.5 wt.% and 72.5 wt.%, respectively. Here, we assume blended cement with 27.5 wt.% carbonation products to perform similarly to conventional OPC and CEM II.

3.4 Scenario definition

Besides the cement substitution, the main economic driver for the implementation of the mineral carbonation process is the participation in the ETS. The carbon prices within the ETS have been increasing steadily and are to increase further within this decade. The current carbon price is forecasted to triple by 2030 compared to 2021.[69] Hence, mineral carbonation economics are expected to strongly improve within the next decade. To evaluate the benefit of an increase in the ETS price, we consider two scenarios: The first one considers current prices for the ETS, utilities, and capital cost to assess the present-day potential of the mineral carbonation process. We calculate the current ETS price as the average of the period July 2020 to July 2021 to a value of 38 €. The second scenario considers the year 2030 with an estimated ETS price of 129 €.[69] Other costs and carbon footprint parameters, e.g., of electricity, are adjusted accordingly for the year of 2030, which is given in the electronic supporting information (ESI). We note that currently the industry is partially subsidized by

allocating ETS certificates at no cost. This cross-funding will be phased down by 2030.[70] Hence, in our study, we do not consider free allocation of ETS certificates.

4 Process optimization

According to Ostovari et al.,[2] carbon-neutral blended cement is technically feasible, however, they did not consider its cost. At the same time, Strunge et al.[15] provided a cost analysis of blended cement and concluded that the scale of the mineral carbonation process is critical for its overall profitability. They find a maximum profit at the plant capacity that enables the highest possible cement substitution with a minimum deposit stream. Yet, this process scale differs from the process scale for carbon-neutral blended cement in Ostovari et al..[2] Therefore, we combine the consideration of both carbon footprint and profitability by using multiobjective Bayesian optimization to determine their trade-off.

In this study, the degrees of freedom for the olivine carbonation process are the reaction temperature, pressure, initial PSD of feedstock material as well as its flow rate into the process. These variables have not yet been determined in a holistic set-up, but rather from a limited point of view, i.e., either from experimental investigations or simplified process models. The feedstock material flow rate is crucial for the overall scale of the process, whereas temperature, pressure, and mean of the PSD of feedstock material determine the overall conversion within the tubular reactors, and hence, the PSDs of solid phases exiting the reactors. We set these degrees of freedom as the decision variables for the optimization and provide lower and upper bounds for the optimizer to find an optimum process.

The scale of the process is limited by the amount of CO_2 production from the cement plant that is available for carbonation, resulting in an upper bound of 800,000 $t_{olivine}$/a. The lower bound for feedstock flow rate is set to 80 wt.% of the required amount for 27.5 wt.% cement substitution, namely 160,000 $t_{olivine}$/a. We expect the process not to be Pareto optimal for a process scale below maximum possible substitution as in this case, both levelized

cost and carbon footprint of SCM increase.[15] We determine the reactor temperature to be within 150 °C and 220 °C, as at lower temperature hydrated magnesium carbonates are observed experimentally[71,72] and at higher temperatures, conversion drops substantially due to a reduced CO_2 solubility.[32] We allow a reactor pressure between 40 bar and 200 bar, as this is the range of operation in experiments. Feedstock particles could be ground to a mean particle size between 5 µm and 30 µm. Lower particle size could hinder separation of magnesite from unreacted olivine particles as magnesite is found in the range of 1 µm to 5 µm.

The optimization formulation has four decision variables: optimal temperature, pressure, mean of feedstock's PSD, and process scale. It is at the border between problems that can be solved with brute-force approaches, such as trivial discretization, and sophisticated optimization methods. Hence, we decided to employ Thompson sampling efficient multiobjective optimization (TSEMO) that enables multiobjective optimization of black-box models based on Gaussian processes (GP) as surrogates.[33] A gradient-based optimization method is not suitable in our case, as we employ a procedural approach of coupling reactor simulation results with the Aspen Plus flowsheet model and do not calculate gradients of the reactor model and the process model. Additionally, the nonsmooth overall model behavior resulting from nucleation within the reactor model and functions for the calculation of levelized cost and carbon footprint does not allow the use of finite differences for the approximation of gradients. Within TSEMO, each optimization is set up by first building an initial GP from the evaluation of objectives by different combinations of optimization variables, i.e., by Latin hypercube design.[73] Subsequently, within the optimization algorithm, an iterative approach of (1) adding sampling points via Thompson sampling (TS), (2) updating the GP with the new data set, (3) multiobjective optimization of the GP with NSGA-II,[74] and (4) an additional process model evaluation yields the Pareto optimal production cost and carbon footprint of blended cement.

The major share of computational time on a PC with an Intel Core i3-6100 CPU for

one iteration is attributed to the integration of the reactor model, as the model incorporates events due to the reinitialization of nodes within the PSDs resulting from nucleation. In total, roughly eight minutes are required to perform one iteration, whereas six minutes are accounted for reactor model integration and two minutes to process simulation. The computational time spent on the optimization algorithm is negligible.

4.1 Optimal operating conditions

Preliminary optimization results show that the particle size is always at its lower bound. Thus, grinding the feedstock particles to a fine powder is beneficial for high conversion rates, which promotes both carbon footprint and profitability. In other words, the higher conversion rates offset the additional GHG emissions and both CapEx and OpEx due to fine grinding. Hence, in the following, we only show optimization results for a fixed mean particle size of feedstock material of 5 µm. Furthermore, to exclude the strong effects of the process scale on both profitability and carbon footprint, we first fix the process size to an SCM production of 275,000 $\frac{\mathrm{t}}{\mathrm{a}}$, which corresponds to the most profitable process scale found by Strunge et al..[15] We found the temperature and pressure dependence on the optimization variables to be orders of magnitude smaller than the process scale dependence on the optimization variables, as evaluated in the following (cf. Figs. 4 and 6).

Hence, we consider only the optimization of temperature and pressure for the first optimization case illustrated in Fig. 4. Pareto optimal temperature and pressure are found after 250 iterations in the range of 195.7-197.6 °C and 165.9-178.2 bar, respectively. Figs. 4a and 4b show the optimization iterations in the design space of temperature and pressure. The color-coded levelized cost and carbon footprint both show that a higher reaction pressure allows a higher temperature, which in return promotes the conversion. A temperature increase is, however, limited by the a reduction of dissolved CO_2 in the liquid phase. Figs. 4c and 4d show the Pareto front with color-coded temperature and pressure, respectively. Increasing the operating pressure increases the carbon footprint of blended cement, and at

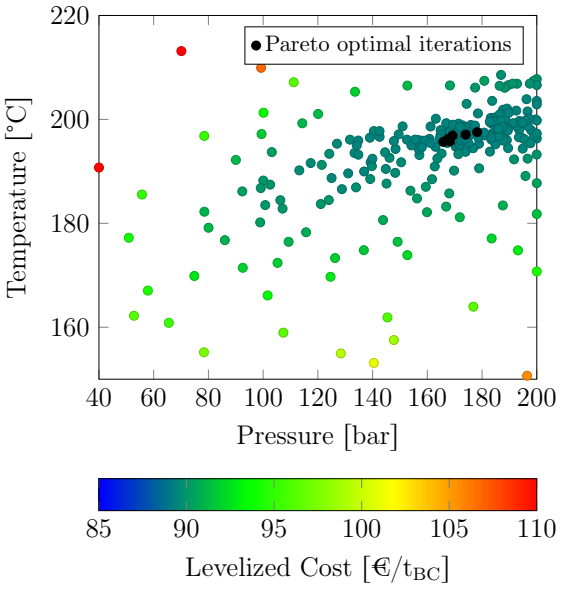

(a) Design space of operating conditions with color-coded levelized cost of blended cement (BC).

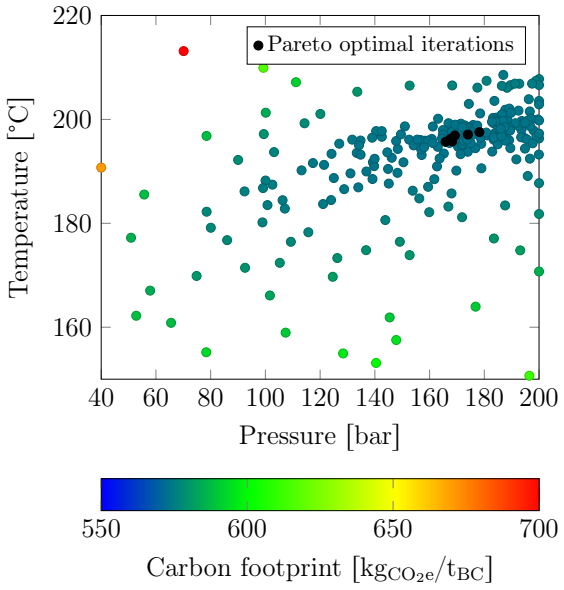

(b) Design space of operating conditions with color-coded carbon footprint of blended cement (BC).

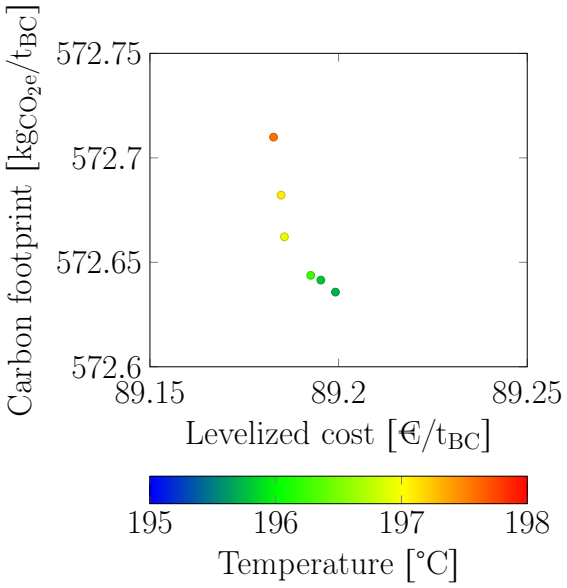

(c) Color-coded temperature on Pareto front.

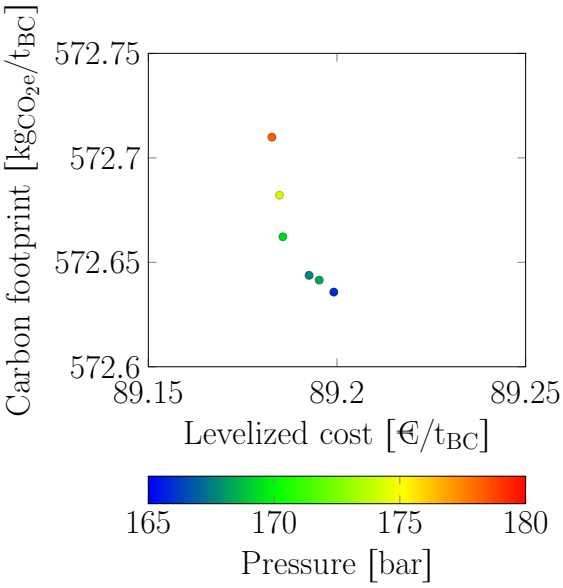

(d) Color-coded pressure on Pareto front.

Figure 4: Influence of temperature and pressure at maximum substitution capacity according to Strunge et al.[15] on (a) levelized cost and (b) carbon footprint with Pareto optimal carbon footprint vs. levelized cost (•). The Pareto front with (c) color-coded Pareto optimal temperature (195.7-197.6 °C) and (d) color coded Pareto optimal pressure (165.9-178.2 bar) show a low trade-off between carbon footprint and levelized cost of blended cement (BC).

the same time, promotes the conversion that reduces the levelized cost (top left of Pareto front). Contrarily, a lower pressure enables a lower carbon footprint at a lower temperature,

but at increased levelized cost (bottom right of Pareto front).

Our results suggest that higher pressures than those argued by O'Connor et al.[19] are feasible and pay off both financially and for the climate. This is the first study to propose a higher pressure than 150 bar for the carbonation of olivine. O'Connor et al.[19] showed improved conversion for higher pressures up to 250 bar, but did not consider this beneficial beyond 150 bar. Still, the direct costs of the compression cascade account for roughly 15 % of the total direct cost and, hence, are a major cost driver of the process. At the same time, high pressure is required for sufficient conversion that is more decisive for a low-emission and profitable process. Therefore, with high pressure and the selection of an appropriate temperature that promotes a high conversion, the levelized cost and the carbon footprint of blended cement are close to the Pareto front. The trade-off between pressure and temperature is then insignificant (cf. Figs. 4a and 4b). In general, carbon footprint and profitability correlate strongly, as participation in the ETS is essential for the profitability of the process. In return, this strong correlation makes the trade-off between Pareto optimal temperature and pressure small (cf. Figs. 4c and 4d).

To put the optimization results into perspective, we compare Pareto optimal processes with process configurations based on operating conditions taken from literature, illustrated in Fig. 5. The lower pressure levels in literature result in lower conversion and, hence, sub-optimal process performance. Nonetheless, the simulation results with literature data must be considered with caution, as the temperature-pressure combinations do not necessarily match the optimal temperature-pressure combinations of the mechanistic reactor model. The differences of levelized cost of blended cement in this work and literature data seem rather low, which is why it is important to note that still, a major share of levelized cost of OPC originates from OPC production as it comprises 72.5 wt.% of the mass of blended cement and only the share of 27.5 wt.% of the SCM production results in the increased cost.

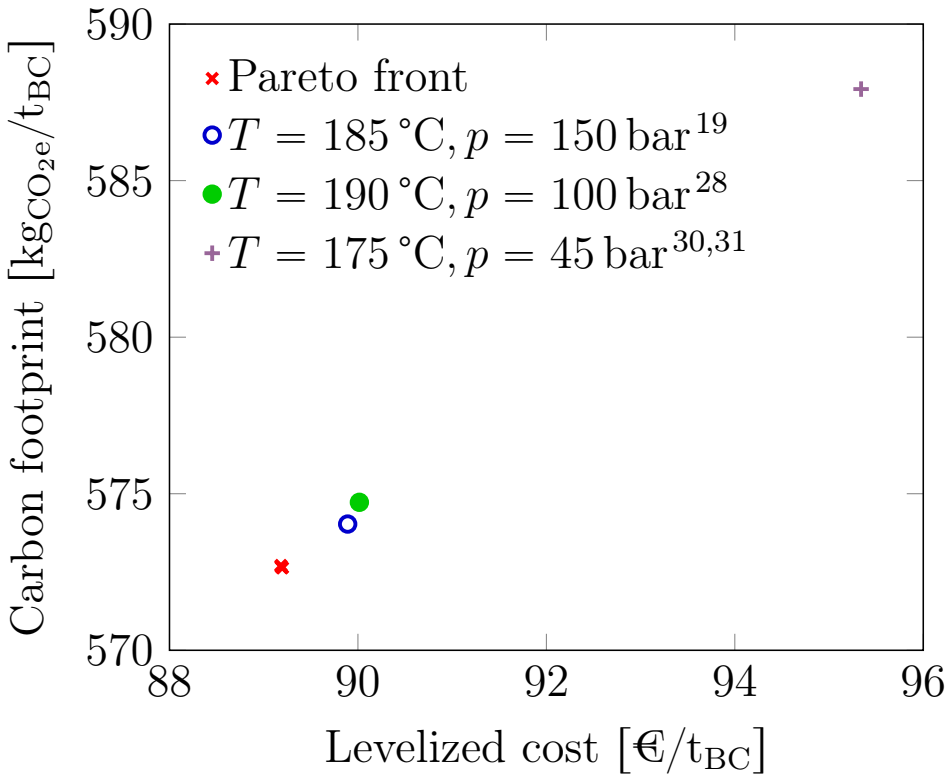

Figure 5: The optimization shows lower carbon footprint and levelized cost of blended cement (BC) compared to simulation with input temperature and pressure taken from literature and a mean particle size of 5 µm.

4.2 Optimal carbonation process scale

To further assess the carbon footprint and cost of blended cement, we consider the optimization of the process scale for the present-day and future scenario. We set the olivine mass flow rate into the process as a decision variable with a predefined lower and upper bound. As the range of Pareto optimal operating conditions has a minor influence on both carbon footprint and levelized cost of blended cement in comparison to process scale, we fix temperature and pressure to one operating condition from the Pareto front of Fig. 4, namely $T = 196.9\,°\mathrm{C}$ and $p = 169.2\,\mathrm{bar}$. Analogous to Section 4.1, we fix the mean particle size of feedstock to 5 µm. With only one decision variable in this optimization scenario, a straightforward discretization is feasible, but the previously employed optimization framework comes at no cost while rendering the same or more accurate results. To benchmark

the produced blended cement from carbonation products with other CEM II on the cement market, we consider CEM II with natural pozzolan. Here, we assume three extreme cases for CEM II with natural pozzolan regarding the carbon footprint of natural pozzolan and its cost, namely natural pozzolan without production cost but the carbon footprint of OPC (CEM II_a), natural pozzolan with the production cost of OPC but carbon footprint equal to zero (CEM II_b), and natural pozzolan without production cost and a carbon footprint of zero (CEM II_c, best-case).

With a total of 100 optimization iterations, the Pareto front illustrated in Fig. 6a shows a trade-off between levelized cost and carbon footprint of blended cement. The carbon footprint of blended cement decreases with increasing process scale as a larger amount of CO_2 is permanently stored by carbonation. The increased amount of stored CO_2 is attributed to blended cement resulting in its lower carbon footprint. In return, the levelized cost of blended cement increases with increasing mineral carbonation process scale, because the amount of utilized SCM from the carbonation process remains constant over the Pareto front. The Pareto front shows several discontinuities resulting from step functions within the total direct cost calculation of the CO_2 compression cascade with the Aspen Capital Cost Estimator. As the CO_2 cascade comprises roughly 15 % of the total direct cost, the discontinuities are visible in the Pareto front.

At minimum levelized cost of blended cement, the process produces as much SCM as can be substituted in blended cement (top left of Pareto front). This represents the most economic process scale illustrated in Fig. 4. An increase in feedstock mass flow rate is still Pareto optimal with an increase of the levelized cost of blended cement and a decrease of the carbon footprint, as more CO_2 from the cement plant is stored. Consequently, the amount of deposited solid products increases. The lowest carbon footprint is found, where the entire amount of available CO_2 from the cement plant is used in the mineral carbonation process. This process configuration decreases the carbon footprint of blended cement down to $456\,\mathrm{kgCO_2e/t_{BC}}$ but increases its levelized cost to $135\,€/\mathrm{t_{BC}}$.

Pareto optimal mineral carbonation capacities result in a generally lower carbon footprint of blended cement than both OPC and CEM II with natural pozzolan in the present day scenario (cf. Fig. 6a). The final product blended cement in the most economic Pareto optimal process configuration is competitive with conventional OPC production while having a lower carbon footprint. The production cost of OPC within the European Union ranges from 35 $\frac{€}{t}$ to 73 $\frac{€}{t}$.[75] In this study, we use a production cost of 62.60 $\frac{€}{t}$.[76] Adding the expenses for ETS certificates in the amount of 32 $\frac{€}{t}$ from 850 $\frac{kg}{t}$ CO_{2e} emissions, the total cost of OPC increases to 95 $\frac{€}{t}$. At a similar levelized cost, the carbon footprint of blended cement is 33 % lower than that of OPC. Considering that OPC and blended cement are categorized as CEM I and CEM II in the European cement standard, respectively, a comparison with the carbon footprint of a comparable CEM II cement is necessary. Assuming zero carbon footprint for natural pozzolan (CEM II_b and CEM II_c in Fig. 6), at the same substitution ratio of OPC with natural pozzolan the carbon footprint of CEM II cement (616 $\frac{kg}{t}$) is still higher than our Pareto optimal results. The carbon footprint reduction in relation to the best case CEM II cement is only 7 %. Hence, the most profitable process scale does not necessarily result in a high carbon footprint reduction. Only an increased process scale enables a reduction of up to 46 % and 26 % compared to OPC and CEM $II_{b/c}$ cement, respectively, by essentially adding carbon storage. In the present day scenario, the carbon footprint of the Pareto optimal mineral carbonation process scale is below the average cement carbon footprint, yet, the levelized cost is beyond present-day cement prices.

As a substantial carbon footprint reduction necessitates considerably increased levelized cost of 135 €/t_{BC}, the realization of the mineral carbonation process seems economically infeasible in the present day scenario due to the lower cost of OPC production. However, with the increasing forecasted ETS price of 129 € in 2030, the cost savings of a carbon footprint reduction should be significant. Without any improvement of the conventional cement process, the levelized costs of both OPC and CEM II are expected to increase due to the increased ETS price (cf. Fig. 6b). We run the process scale optimization again

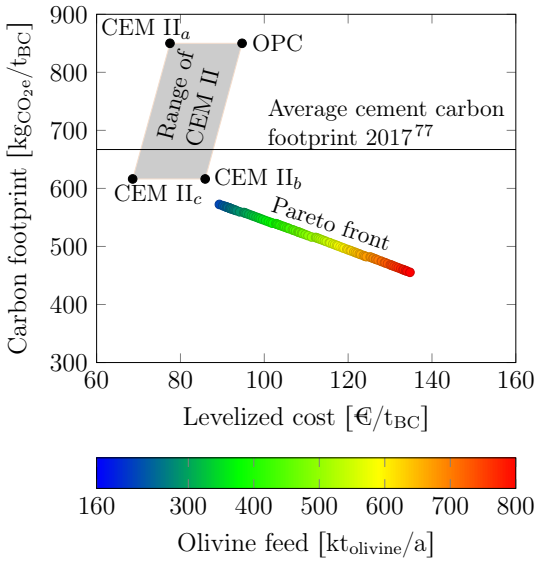

(a) Present day scenario (2021).

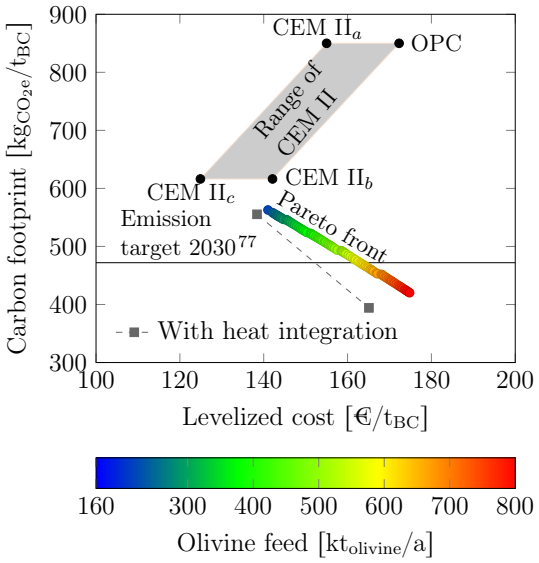

(b) Future scenario (2030). Additionally, we show heat integrated results of the minimum and maximum Pareto optimal process capacity and interpolate - ■- .

Figure 6: Pareto optimal carbon footprint and levelized cost of blended cement with olivine feed as a decision variable for (a) the present day scenario (2021) and (b) the future scenario (2030). The top left of both Pareto fronts represent the process scale at maximum substitution, the bottom right of the Pareto fronts shows the limit of CO_2 availability from the cement process. The range of conventional CEM II is derived from cement blends containing 72.5 % OPC and 27.5 % of SCM with (CEM II$_a$) no production cost and carbon footprint of OPC, (CEM II$_b$) production cost of OPC and zero carbon footprint, and (CEM II$_c$) no production cost and zero carbon footprint.

with cost estimations for 2030 and the same operating conditions as in the present day scenario, since the influence of operating conditions is rather low. The results illustrated in Fig. 6b show an increased Pareto optimal levelized cost of blended cement, while the carbon footprint is further reduced due to a lower carbon footprint of utilities. Again, the most profitable process scale is found at maximum substitution capacity (top left in the graph). The largest carbon footprint reduction is 51 % and 32 % compared to OPC production and the best case CEM II production, respectively. In comparison to the present day scenario, a process scale increase is less costly, as can be seen from the steeper decrease of the Pareto front for the future scenario. This stems from the increased ETS price, which makes the mineral carbonation process scale-up less expensive compared to the present-day scenario.

The Pareto optimal levelized costs of blended cement are in the range of cost for OPC and CEM II, which shows the economic feasibility of combined cement and SCM production via mineral carbonation. Furthermore, by employing mineral carbonation in the cement industry, the emission targets of 472 kg_{CO_2e}/t_{BC} [77] could be met. This underlines the future capabilities of applying mineral carbonation products in the cement industry. We underline that mineral carbonation as a stand-alone process without the application of its products in the cement industry becomes economically feasible only at an ETS price of 327 € (cf. Appendix C). Hence, the use of mineral carbonation products as SCM is essential to achieve an economic process configuration by 2030.

4.2.1 Heat integration for further process improvement

A high share of costs and GHG emissions of mineral carbonation stems from utility demand (Tabs. 6 and 7 of Appendix C) Therefore, the effect of heat integration on cost and GHG emissions of mineral carbonation can be strong. A priori, we manually integrated the excess heat from the reactor to the required heat for the MEA post-combustion capture, and heat up the solid-liquid reactor feed slurry with the reactor outflow. Within the optimization algorithm, we did not perform a complete heat integration. A pinch analysis of the remaining hot and cold streams results in a decrease of utility cost by 18 % and 11 % for the minimum and maximum Pareto optimal mineral carbonation capacity, respectively, considering the future scenario (2030). Without consideration of potential additional CapEx, this results in a reduction of carbon footprint and levelized cost of blended cement to 555 kg_{CO_2e}/t_{BC} and 138 €/t_{BC} for the lowest Pareto optimal process capacity, respectively. Heat integration at the largest Pareto optimal process scale results in a carbon footprint and levelized cost of 394 kg_{CO_2e}/t_{BC} and 165 €/t_{BC}, respectively. These results are illustrated in Fig. 6b and interpolated for process capacities that lie within the lowest and largest Pareto optimal capacity. In summary, the consideration of heat integration in the future scenario allows a carbon footprint reduction of 54 % and 36 % compared to OPC and best case CEM II

production, respectively.

5 Conclusion and outlook

In this work, we combined process modeling and Bayesian optimization to evaluate the capabilities of mineral carbonation to reduce the carbon footprint of the cement industry while ensuring the economic competitiveness of the process. For this purpose, we proposed a mineral carbonation process with an integrated tubular mineral carbonation reactor. The mineral carbonation process model was implemented in Aspen Plus and coupled with a mechanistic tubular reactor model implemented in Modelica. We defined an application for mineral carbonation products in the cement industry for the production of CEM II cement. With models both for the carbon footprint and the cost of the produced blended cement, we evaluated the mineral carbonation process producing SCM for the cement industry. By the use of Bayesian optimization, we found Pareto optimal operating conditions for the mineral carbonation reactor and the process scale.

Our results showed that the carbon footprint and cost of the mineral carbonation process were at their minimum for a mean particle size of the feedstock of 5 µm, a temperature range of 196-198 °C, and a pressure range of 166-178 bar. The Pareto optimal process scale showed a strong trade-off between carbon footprint and cost. The stored CO_2 is directly attributed to overall CO_2 emissions of blended cement resulting in a lower carbon footprint with increasing process scale. Similarly, the higher cost of a larger process scale is attributed to the cost of blended cement, thus increasing its levelized cost. Today's production of blended cement was most competitive at maximum substitution capacity with a carbon footprint reduction of 33 % and 7 % compared to the carbon footprint of OPC and best case CEM II, respectively. In the future scenario (2030), mineral carbonation can produce a blended cement with 51 % lower carbonation footprint at a competitive cost. Heat integration of the mineral carbonation process can reduce the carbon footprint further by 54 % at a lower

levelized cost than that of OPC. With this process configuration, the emission targets for 2030 can be significantly undercut.

The foundation of these results was given by rigorous process modeling with the use of mechanistic modeling of a multi-phase tubular reactor. However, the reactor model still may contain inaccuracies, which need further consideration, as the conversion is crucial for a low-emission and cost-efficient process. Still, the mechanistic tubular reactor model is a first step towards underlining the potential of applying tubular reactors in an industrial-scale mineral carbonation process. Furthermore, the downstream process for the solid separation is designed for the properties of solid phases that are computed by the reactor model. As the mechanistic model does not account for solid particle interaction, the downstream process that is based on previous work should be considered closely. Nonetheless, the downstream process is designed at ambient conditions and requires small amounts of utilities compared to upstream units. Hence, the downstream units cause only a minor share of CapEx, OpEx, and GHG emissions. Thus, design changes are not expected to have a major influence on the optimization results.

While process and reactor modeling are still subject to further investigation, this work highlights the potential of applying mineral carbonation in the cement industry. Next to the process set-up, the applicability of SCM from mineral carbonation in blended cement requires an in-depth evaluation. Policymaking for the standardization of mineral carbonation products as well as progress towards participation in the ETS are the basis for the future implementation of an industrial scale mineral carbonation process.

Supporting Information Available

We provide process models that are required for the process evaluation. The files are provided in a .zip folder in the following structure:

- Document: Supporting Information with data and calculations for reactor modeling,

scenario data, and the stand-alone mineral carbonation process.

- AspenPlus: AspenPlus process model and ASW Excel file
- Dymola: Modelica code and executable for reactor simulation
- Matlab: Functions for calling reactor and process model for the evaluation of carbon footprint and levelized cost
- Results: Folder structure for saving simulation results

This information is available free of charge via the Internet at `http://pubs.acs.org/`

Acknowledgement

We thank the Federal Ministry of Education and Research (BMBF) for funding of the project CO2Min (033RO14B).

A Data and calculations for reactor modeling

In Tab. 1, we provide the design specifications of a tubular reactor that we employ for the mineral carbonation reaction. We use this data to determine flow regimes of the slurry and the gas phase flow with results provided in Tab. 2. To underline the separate flow of gas and slurry flow, we provide the calculations for the determination of flow patterns in Tab. 3 and refer to the corresponding graphs by Baker,[43] who provided the groundwork for the prediction of two-phase flow patterns. The results are in accordance with a more recent study.[78]

Table 1: Reactor design properties.

Specification	Value
Length L	120 m
Diameter d	1.25 m
Residence time τ	3 h
Volume flow $\dot{V}$	$1.36 \times 10^{-2}\ \frac{\mathrm{m}^3}{\mathrm{s}}$
Flow velocity v	$0.011\ \frac{\mathrm{m}}{\mathrm{s}}$
Volume share of gas phase	10 %
Hydraulic diameter gas flow d_h	0.24 m
Hydraulic diameter slurry flow d_h	0.76 m

Table 2: Reactor flow properties at 185 °C and 150 bar.

Substance	Density $\left[\frac{\mathrm{kg}}{\mathrm{m}^3}\right]$	Viscosity [mPa s]	d_h [m]	$Re = \frac{\rho v d_h}{\eta}$ [−]	$Bo = \frac{vL}{D_{ax}}$ [−]
Water	890.8 [79]	0.149 [79]	-	-	-
Olivine	3223 [80]	-	-	-	-
Suspension ($0.2\ \mathrm{kg_{olivine}/kg_{water}}$)	1013	0.172 [40]	0.76	4.9×10^4	6.1×10^2
Gas (CO_2/H_2O)	194.1 [81]	0.0215 [82]	0.24	2.4×10^4	-

Table 3: Flow pattern according to Baker. [43]

Specification	Value
$\frac{G_g}{\lambda}$	$0.017\ \frac{\mathrm{kg\,s}}{\mathrm{m}^2}$
$\frac{G_l \lambda \Phi}{G_g}$	1084

B Present day and future scenario data

In Tabs. 4 and 5, we provide relevant data for the cost and GHG emission calculations. Here, we present the changed values in the present day and future scenario. For further detail on parameters and data, we refer to Strunge et al. [15] for the techno-economic assessment and

to Ostovari et al.[2] for the life cycle assessment.

Table 4: Price data for techno-economic assessment.

Scenario	Present day (2021)	Future (2030)
EU ETS [€/t_{CO_2}]	37.73[83]	129[69]
Electricity [$\frac{€}{MWh}$]	58.1[84]	62[85]
Natural gas [$\frac{€}{MWh}$]	21.6[86]	32[87]

Table 5: GHG emission data.[88]

Scenario	Present day (2021)	Future (2030)
Electricity [$kg_{CO_{2e}}$/kWh]	0.4	0.208
Steam [$kg_{CO_{2e}}$/kWh]	0.24	0.219

C Stand-alone mineral carbonation process

In addition to the approach of combining cement production and mineral carbonation to produce SCM, mineral carbonation also offers the possibility of a stand-alone unit. In this case, the purpose of mineral carbonation is solely the storage of CO_2 in a solid material without a substitution of cement. In this section, we provide carbon footprint and cost data of a stand-alone mineral carbonation process for the future scenario (2030). Here, the products of mineral carbonation are not substituting OPC. Thus, we consider only the large-scale process of 800,000 $t_{olivine}$/a that uses the available CO_2 from the cement process with a production capacity of 725,000 t_{OPC}/a. The CO_2 mitigation cost are calculated to 327 €/$t_{CO_2 avoided}$ with a total of 231,000 $t_{CO_2 avoided}$/a and 370,000 $t_{CO_2 stored}$/a. The cost distribution is given in Tab. 6, which is similar to the results of Strunge et al..[15] Tab. 7 provides the distribution of GHG emissions resulting from the process. The utilities show a major share of carbon footprint while the feedstock procurement (mining) has a negligible influence.

Table 6: Cost distribution of a stand-alone mineral carbonation process with a capacity of 800,000 $t_{olivine}$/a.

Position	Share [%]
Utilities	42.8
Feedstock	13.3
Transportation	13.6
Annualized CapEx	19.6
Fixed OpEx	10.7

Table 7: Distribution of GHG emissions of a stand-alone mineral carbonation process with a capacity of 800,000 $t_{olivine}$/a.

Position	Share [%]
Utilities	78.0
Feedstock	0.3
Transportation	15.9
Construction	5.8

References

(1) IEA, Transforming Industry through CCUS. 2019; `https://www.iea.org/reports/transforming-industry-through-ccus` (last visited March 4, 2021).

(2) Ostovari, H.; Müller, L.; Skocek, J.; Bardow, A. From Unavoidable CO2 Source to CO2 Sink? A Cement Industry Based on CO2 Mineralization. *Environ. Sci. Technol.* **2021**, *55*, 5212–5223.

(3) Schneider, M.; Romer, M.; Tschudin, M.; Bolio, H. Sustainable cement production—present and future. *Cem. Concr. Res.* **2011**, *41*, 642–650.

(4) Atmaca, A.; Kanoglu, M. Reducing energy consumption of a raw mill in cement industry. *Energy* **2012**, *42*, 261–269.

(5) Karellas, S.; Leontaritis, A.-D.; Panousis, G.; Bellos, E.; Kakaras, E. Energetic and exergetic analysis of waste heat recovery systems in the cement industry. *Energy* **2013**, *58*, 147–156.

(6) Mikulčić, H.; Klemeš, J. J.; Vujanović, M.; Urbaniec, K.; Duić, N. Reducing greenhouse

gasses emissions by fostering the deployment of alternative raw materials and energy sources in the cleaner cement manufacturing process. *J. Clean. Prod.* **2016**, *136*, 119–132.

(7) Habert, G.; Miller, S. A.; John, V. M.; Provis, J. L.; Favier, A.; Horvath, A.; Scrivener, K. L. Environmental impacts and decarbonization strategies in the cement and concrete industries. *Nat. Rev. Earth Environ.* **2020**, *1*, 559–573.

(8) Barker, D. J.; Turner, S. A.; Napier-Moore, P. A.; Clark, M.; Davison, J. E. CO2 Capture in the Cement Industry. *Energy Procedia* **2009**, *1*, 87–94.

(9) Bosoaga, A.; Masek, O.; Oakey, J. E. CO2 Capture Technologies for Cement Industry. *Energy Procedia* **2009**, *1*, 133–140.

(10) Hills, T.; Leeson, D.; Florin, N.; Fennell, P. Carbon Capture in the Cement Industry: Technologies, Progress, and Retrofitting. *Environ. Sci. Technol.* **2016**, *50*, 368–377.

(11) Paris, J. M.; Roessler, J. G.; Ferraro, C. C.; DeFord, H. D.; Townsend, T. G. A review of waste products utilized as supplements to Portland cement in concrete. *J. Clean. Prod.* **2016**, *121*, 1–18.

(12) Bui, M. et al. Carbon capture and storage (CCS): the way forward. *Energy Environ. Sci.* **2018**, *11*, 1062–1176.

(13) Seifritz, W. CO_2 disposal by means of silicates. *Nature* **1990**, *345*, 486.

(14) Ostovari, H.; Sternberg, A.; Bardow, A. Rock 'n' use of CO 2: Carbon footprint of carbon capture and utilization by mineralization. *Sustain. Energy Fuels* **2020**, *50*, 1004.

(15) Strunge, T.; Renforth, P.; van der Spek, M. Towards a business case for CO2 mineralisation in the cement industry. *Commun. Earth Environ.* **2022**, *3*, 2141.

(16) Benhelal, E.; Rashid, M. I.; Holt, C.; Rayson, M. S.; Brent, G.; Hook, J. M.; Stockenhuber, M.; Kennedy, E. M. The utilisation of feed and byproducts of mineral carbonation processes as pozzolanic cement replacements. *J. Clean. Prod.* **2018**, *186*, 499–513.

(17) Lackner, K. S. Carbonate chemistry for sequestring fossil carbon. *Annu. Rev. Energy. Environ.* **2002**, *27*, 193–232.

(18) Huijgen, W.; Comans, R. Carbon dioxide sequestration by mineral carbonation Literature Review update 2003-2004. 2005; `http://inis.iaea.org/search/search.aspx?orig_q=RN:37083921`.

(19) O'Connor, W.; Dahlin, D. C.; Rush, G. E.; Gerdemann, S. J. Aqueous Mineral Carbonation: Mineral Availability, Pretreatment, Reaction Parametrics, And Process Studies. 2005.

(20) Gerdemann, S. J.; O'Connor, W.; Dahlin, D. C.; Penner, L. R.; Rush, H. Ex situ aqueous mineral carbonation. *Environ. Sci. Technol.* **2007**, *41*, 2587–2593.

(21) Naraharisetti, P. K.; Yeo, T. Y.; Bu, J. New classification of CO2 mineralization processes and economic evaluation. *Renew. Sustain. Energy Rev.* **2019**, *99*, 220–233.

(22) Hitch, M.; Dipple, G. M. Economic feasibility and sensitivity analysis of integrating industrial-scale mineral carbonation into mining operations. *Miner. Eng.* **2012**, *39*, 268–275.

(23) Siwior, P.; Bukowska, J. Commentary on European Court of Justice judgement of 19 January 2017 in case C-460/15 Schaefer Kalk GmbH & Co. KG v Bundesrepublik Deutschland. *Environmental Protection and Natural Resources* **2018**, *29*, 25–30.

(24) Haug, T. A. Dissolution and carbonation of mechanically activated olivine: Investigating CO_2 sequestration possibilities. Dissertation, Norwegien University of Science and Technology, Trondheim, 2010.

(25) Gadikota, G.; Swanson, E. J.; Zhao, H.; Park, A.-H. A. Experimental Design and Data Analysis for Accurate Estimation of Reaction Kinetics and Conversion for Carbon Mineralization. *Ind. Eng. Chem. Res.* **2014**, *53*, 6664–6676.

(26) Gadikota, G.; Matter, J.; Kelemen, P.; Park, A.-H. A. Chemical and morphological changes during olivine carbonation for CO_2 storage in the presence of NaCl and $NaHCO_3$ 3. *Phys. Chem. Chem. Phys.* **2014**, *16*, 4679–4693.

(27) Gadikota, G. Commentary: Ex Situ Aqueous Mineral Carbonation. *Front. Energy Res.* **2016**, *4*, 4802.

(28) Eikeland, E.; Blichfeld, A. B.; Tyrsted, C.; Jensen, A.; Iversen, B. B. Optimized carbonation of magnesium silicate mineral for CO2 storage. *ACS Appl. Mater. Interfaces.* **2015**, *7*, 5258–5264.

(29) Rahmani, O.; Highfield, J.; Junin, R.; Tyrer, M.; Pour, A. B. Experimental Investigation and Simplistic Geochemical Modeling of CO_2 Mineral Carbonation Using the Mount Tawai Peridotite. *Molecules* **2016**, *21*, 353.

(30) Wang, F.; Dreisinger, D.; Jarvis, M.; Hitchins, T. Kinetics and mechanism of mineral carbonation of olivine for CO2 sequestration. *Miner. Eng.* **2019**, *131*, 185–197.

(31) Wang, F.; Dreisinger, D.; Jarvis, M.; Hitchins, T.; Dyson, D. Quantifying kinetics of mineralization of carbon dioxide by olivine under moderate conditions. *Chem. Eng. J.* **2019**, *360*, 452–463.

(32) Bremen, A. M.; Ploch, T.; Mhamdi, A.; Mitsos, A. A mechanistic model of direct forsterite carbonation. *Chem. Eng. J.* **2021**, *404*, 126480.

(33) Bradford, E.; Schweidtmann, A. M.; Lapkin, A. Efficient multiobjective optimization employing Gaussian processes, spectral sampling and a genetic algorithm. *J. Glob. Optim.* **2018**, *71*, 407–438.

(34) Pasquier, L.-C.; Mercier, G.; Blais, J.-F.; Cecchi, E.; Kentish, S. Technical & economic evaluation of a mineral carbonation process using southern Québec mining wastes for CO2 sequestration of raw flue gas with by-product recovery. *Int. J. Greenh. Gas Control* **2016**, *50*, 147–157.

(35) Kremer, D.; Wotruba, H. Separation of Products from Mineral Sequestration of CO2 with Primary and Secondary Raw Materials. *Minerals* **2020**, *10*, 1098.

(36) Turri, L.; Muhr, H.; Rijnsburger, K.; Knops, P.; Lapicque, F. CO2 sequestration by high pressure reaction with olivine in a rocking batch autoclave. *Chem. Eng. Sci.* **2017**, *171*, 27–31.

(37) Santos, R. M.; Knops, P. C. M.; Rijnsburger, K. L.; Chiang, Y. W. CO2 Energy Reactor – Integrated Mineral Carbonation: Perspectives on Lab-Scale Investigation and Products Valorization. *Front. Energy Res.* **2016**, *4*.

(38) Kremer, D.; Etzold, S.; Boldt, J.; Blaum, P.; Hahn, K. M.; Wotruba, H.; Telle, R. Geological Mapping and Characterization of Possible Primary Input Materials for the Mineral Sequestration of Carbon Dioxide in Europe. *Minerals* **2019**, *9*, 485.

(39) Myers, C. A.; Nakagaki, T.; Akutsu, K. Quantification of the CO2 mineralization potential of ironmaking and steelmaking slags under direct gas-solid reactions in flue gas. *Int. J. Greenh. Gas Control* **2019**, *87*, 100–111.

(40) Thomas, D. G. Transport characteristics of suspension: VIII. A note on the viscosity of Newtonian suspensions of uniform spherical particles. *J. Colloid Sci.* **1965**, *20*, 267–277.

(41) Stopic, S.; Dertmann, C.; Koiwa, I.; Kremer, D.; Wotruba, H.; Etzold, S.; Telle, R.; Knops, P.; Friedrich, B. Synthesis of Nanosilica via Olivine Mineral Carbonation under High Pressure in an Autoclave. *Metals* **2019**, *9*, 708.

(42) Aspen Technology, Aspen Icarus Reference Guide - Icarus Evaluation Engine (IEE) V8.0. 2012.

(43) Baker, O. Design of Pipelines for the Simultaneous Flow of Oil and Gas. *Oil Gas J.* **1954**, *1*, 185–195.

(44) Cussler, E. L. *Diffusion: Mass transfer in fluid systems*, 3rd ed.; Cambridge Univ. Press: Cambridge, 2011.

(45) Taylor, G. The dispersion of matter in turbulent flow through a pipe. *Proc. R. Soc. Lond. A* **1954**, *223*, 446–468.

(46) Rumble, J. R., Ed. *CRC handbook of chemistry and physics*, 102nd ed.; CRC Press: Boca Raton and London and New York, 2021.

(47) Moe, H. I.; Hauan, S.; Lien, K. M.; Hertzberg, T. Dynamic model of a system with phase- and reaction equilibrium. *Comput. Chem. Eng.* **1995**, *19*, 513–518.

(48) Kumar, S.; Ramkrishna, D. On the solution of population balance equations by discretization - III. Nucleation, growth and aggregation of particles. *Chem. Eng. Sci.* **1997**, *52*, 4659–4679.

(49) Vora, N.; Daoutidis, P. Nonlinear model reduction of chemical reaction systems. *AIChE J.* **2001**, *47*, 2320–2332.

(50) Daoutidis, P. In *Surveys in differential-algebraic equations*; Ilchmann, A., Reis, T., Eds.; Differential-algebraic equations forum, DAE-F; Springer: Cham, 2015; pp 69–102.

(51) Aspen Technology Inc., Aspen Plus. 2021; `https://www.aspentech.com/en/products/engineering/aspen-plus`.

(52) Dassault Systèmes AB, Dymola: Dynamic Modeling Laboratory. 2020; `https://www.3ds.com/products-services/catia/products/dymola/`.

(53) Modelica Association, Modelica. 2021; https://www.modelica.org/.

(54) Caspari, A.; Bremen, A. M.; Faust, J.; Jung, F.; Kappatou, C. D.; Sass, S.; Vaupel, Y.; Hannemann-Tamás, R.; Mhamdi, A.; Mitsos, A. *29th European Symposium on Computer Aided Process Engineering*; Computer Aided Chemical Engineering; Elsevier, 2019; Vol. 46; pp 619–624.

(55) The MathWorks, I. Matlab 2019b. 2021; https://www.mathworks.com/products/matlab.html.

(56) Microsoft Corporation, Microsoft Excel 2016. 2021; https://office.microsoft.com/excel.

(57) Petzold, L. R. *A description of DASSL: A differential/algebraic system solver*; SAND82-8637; Sandia National Laboratories, 1982.

(58) Deutsches Institut für Normung e.V., Cement - Part 1: Composition, specifications and conformity criteria for common cements; German version. 2011.

(59) CEMBUREAU, Cements for a low-carbon Europe: A review of the diverse solutions applied by the European cement industry through clinker substitution to reducing the carbon footprint of cement and concrete in Europe. 2012.

(60) Favier, A.; de Wolf, C.; Scrivener, K.; Habert, G. A sustainable future for the European Cement and Concrete Industry: Technology assessment for full decarbonisation of the industry by 2050. 2018.

(61) Valderrama, C.; Granados, R.; Cortina, J. L.; Gasol, C. M.; Guillem, M.; Josa, A. Implementation of best available techniques in cement manufacturing: a life-cycle assessment study. *J. Clean. Prod.* **2012**, *25*, 60–67.

(62) Sanna, A.; Uibu, M.; Caramanna, G.; Kuusik, R.; Maroto-Valer, M. M. A review of

mineral carbonation technologies to sequester CO_2. *Chem. Soc. Rev.* **2014**, *43*, 8049–8080.

(63) Rubin, E. S. Improving cost estimates for advanced low-carbon power plants. *Int. J. Greenh. Gas Control* **2019**, *88*, 1–9.

(64) Roussanaly, S.; Berghout, N.; Fout, T.; Garcia, M.; Gardarsdottir, S.; Nazir, S. M.; Ramirez, A.; Rubin, E. S. Towards improved cost evaluation of Carbon Capture and Storage from industry. *Int. J. Greenh. Gas Control* **2021**, *106*, 103263.

(65) ISO 14040:2006, Environmental management - Life cycle assessment - Principles and framework. 2006.

(66) ISO 14044:2006, Environmental management - Life cycle assessment - Requirements and guidelines. 2006.

(67) ISO 14067:2018, Greenhouse gases - Carbon footprint of products - Requirements and guidelines for quantification. 2018.

(68) Müller, L. J.; Kätelhön, A.; Bringezu, S.; McCoy, S.; Suh, S.; Edwards, R.; Sick, V.; Kaiser, S.; Cuéllar-Franca, R.; El Khamlichi, A.; Lee, J. H.; von der Assen, N.; Bardow, A. The carbon footprint of the carbon feedstock CO 2. *Energy Environ. Sci.* **2020**, *13*, 2979–2992.

(69) Pietzcker, R. C.; Osorio, S.; Rodrigues, R. Tightening EU ETS targets in line with the European Green Deal: Impacts on the decarbonization of the EU power sector. *Appl. Energy* **2021**, *293*, 116914.

(70) International Carbon Action Partnership, EU Emissions Trading Syystem (EU ETS). 2021; `https://icapcarbonaction.com/en/?option=com_etsmap&task=export&format=pdf&layout=list&systems%5B%5D=43`.

(71) Pan, S.-Y.; Ling, T.-C.; Park, A.-H. A.; Chiang, P.-C. An Overview: Reaction Mechanisms and Modelling of CO_2 Utilization via Mineralization. *Aerosol Air Qual. Res.* **2018**, *18*, 829–848.

(72) Hänchen, M.; Prigiobbe, V.; Baciocchi, R.; Mazzotti, M. Precipitation in the Mg-carbonate system-effects of temperature and CO_2 pressure. *Chem. Eng. Sci.* **2008**, *63*, 1012–1028.

(73) Stein, M. Large Sample Properties of Simulations Using Latin Hypercube Sampling. **1987**, *29*, 143–151.

(74) Deb, K.; Pratap, A.; Agarwal, S.; Meyarivan, T. A fast and elitist multiobjective genetic algorithm: NSGA-II. *IEEE Trans. Evol. Computat.* **2002**, *6*, 182–197.

(75) European Commission, Competitiveness of the European Cement and Lime Sectors: Final report. 2018; `https://ec.europa.eu/growth/publications/competitiveness-european-cement-and-lime-sectors_en`.

(76) Voldsund, M.; Anantharaman, R.; Berstad, D.; Fu, C.; Gardarsdottir, S.; Jamali, A.; Perez-Caivo, J.; Romano, M.; Roussanaly, S.; Ruppert, J. CEMCAP Comparative Techno-Economic Analysis of CO2 Capture in Cement Plants (D4. 6). 2018; `https://zenodo.org/record/2597091`.

(77) CEMBUREAU, Cementing the European Green Deal: Reaching climate neutrality along the cement and concrete calue chain by 2050. 2020; `https://cembureau.eu/library/reports/2050-carbon-neutrality-roadmap/`.

(78) Barnea, D.; Shoham, O.; Taitel, Y.; Dukler, A. E. Flow pattern transition for gas-liquid flow in horizontal and inclined pipes. Comparison of experimental data with theory. *Int. J. Multiph. Flow* **1980**, *6*, 217–225.

(79) Wagner, W., Kretzschmar, H.-J., Eds. *International Steam Tables*; Springer Berlin Heidelberg: Berlin, Heidelberg, 2008.

(80) Holland, T. J. B.; Powell, R. An improved and extended internally consistent thermodynamic dataset for phases of petrological interest, involving a new equation of state for solids. *J. Metamorph. Geol.* **2011**, *29*, 333–383.

(81) Peng, D.-Y.; Robinson, D. B. A New Two-Constant Equation of State. *Ind. Eng. Chem. Fund.* **1976**, *15*, 59–64.

(82) Poling, B. E.; Prausnitz, J. M.; O'Connell, J. P. *Properties of Gases and Liquids, Fifth Edition*, fifth edition ed.; McGraw-Hill's AccessEngineering; McGraw-Hill Education and McGraw Hill: New York, N.Y., 2020.

(83) European Energy Exchange AG, EUA Emission Spot Primary Market Auction Report. 2021; `https://www.eex.com/en/market-data/environmental-markets/eua-primary-auction-spot-download`.

(84) Anantharaman, R.; Berstad, D.; Cinti, G.; de Lena, E.; Gatti, M.; Hoppe, H.; Martinez, I.; Monterio, J. G. M.-S.; Romano, M.; Roussanaly, S.; Schols, E.; Spinelli, M.; Størset, S.; van Os, P.; Voldsund, M. Cemcap Framework For Comparative Techno-Economic Analysis Of CO_2 Capture From Cement Plants - D3.2. 2018.

(85) European Commission, Communication from the commission to the European Parliament, the Council, the European Economic and Social Committee and the Committee of the regions: Energy prices and costs in Europe. 2019.

(86) K. Koring, V. Hoenig, H. Hoppe, J. Horsch, C. Suchak, V. Klevenz, B. Emberger, *Deployment of CCS in the Cement Industry*; IEAGHG, 2013.

(87) I. Duić, N. Štefanić, Z. Lulić,G. Krajačić, T. Pukšec, T. Novosel, EU28 fuel prices

for 2015, 2030 and 2050. Deliverable 6.1: Future fuel price review. 2017; https://scholar.google.de/citations?user=ysyxxuiaaaaj&hl=de&oi=sra.

(88) Thinkstep AG, GaBi 9.2, Software-System and Database for Life. 2019.

Graphical TOC Entry